APPENDIX S1

Contents

Derivation of limiting case predictions for synchrony of per capita growth rates (Equations 3-4) 4

Materials and methods details 8

Vital rate statistical models 8

Multi-species populations models 9

Results for synchrony of percent cover 11

Supporting Figures 12

Supporting Tables 18

Interaction Coefficients for Vital Rates in Arizona 19

Interaction Coefficients for Vital Rates in Idaho 20

Interaction Coefficients for Vital Rates in Kansas 21

Interaction Coefficients for Vital Rates in Montana 22

Interaction Coefficients for Vital Rates in New Mexico 23

References 24

List of Figures

S1 Observed (vertical dashed lines) and simulated (solid density curves) synchrony of species per capita growth rates at each site from the IBM (top panels) and the IPM (bottom panels). IPM density curves come from 100 random contiguous sections from 2,000 iteration IPM runs, where the length of each randomly selected section is equal to the number of observation years for each data set. IBM density curves come from 100 replicate simulations of 75 iterations each. Synchrony values come from simulations where environmental stochasticity and interspecific interactions are present. The IBM was run on a 5 by 5 meter landscape to reduce the effect of demographic stochasticity. 12

S2 Community-wide synchrony of species percent cover from model simulation experiments. Synchrony of species' percent cover for each study area are from simulation experiments with demographic stochasticity, environmental stochasticity, and interspecific competition present ("All Drivers"), demographic stochasticity removed ("No D.S."), environmental stochasticity removed ("No E.S."), interspecific competition removed ("No Comp."), interspecific competition and demographic stochasticity removed ("No Comp. + No D.S."), and interspecific competition and environmental stochasticity removed ("No Comp. + No E.S."). Abbreviations within the bars for the New Mexico site indicate whether the IBM or IPM was used for a particular simulation. Error bars represent the 2.5% and 97.5% quantiles from model simulations. 13

S3 Synchrony of species' percent cover for each study area from IBM simulations across different landscape sizes when only demographic stochastcity is present ("D.S. Only") and when environmental stochasticity is also present removed ("D.S. + E.S."). The horizontal lines show the analytical predictions $\mathcal{M}_D$ (dashed line) and $\mathcal{M}_E$ (dotted line). The strength of demographic stochasticity decreases as landscape size increases because population sizes also increase. Error bars represent the 2.5% and 97.5% quantiles from model simulations. 14

S4 Variance of percent cover for each species (along x-axes) in each site through time from simulations with only environmental stochasticity operating (IPM with no species interactions). 15

S5 Variance of per capita growth rates for each species (along x-axes) in each site through time from simulations with only environmental stochasticity operating (IPM with no species interactions). 15

S6 Variance of percent cover for each species (along x-axes) in each site through time from simulations with only demographic stochasticity operating (IBM simulated on 5 by 5 meter landscape). 16

S7 Variance of per capita growth rates for each species (along x-axes) in each site through time from simulations with only demographic stochasticity operating (IBM simulated on 5 by 5 meter landscape). 16

S8 Community-wide synchrony of species' growth rates from model simulation experiments for the Idaho community with *Artemisia tripartita* removed. Synchrony of species' growth rates are from simulation experiments with demographic stochasticity, environmental stochasticity, and interspecific competition present ("All Drivers"), demographic stochasticity removed ("No D.S."), environmental stochasticity removed ("No E.S."), interspecific competition removed ("No Comp."), interspecific competition and demographic stochasticity removed ("No Comp. + No D.S."), and interspecific competition and environmental stochasticity removed ("No Comp. + No E.S."). Error bars represent the 2.5% and 97.5% quantiles from model simulations. 17

List of Tables

S1 Comparisons between our analytical predictions and simulation results for synchrony of species' per capita growth rates. Analytical predictions represent two limiting cases where only demographic stochasticity is operating ($\phi_{R,\mathcal{M}_D}$) and where only environmental stochasticity is operating ($\phi_{R,\mathcal{M}_E}$). Simulated synchrony values come from our empirically-based, multi-species population models when simulated under conditions that match the limiting case conditions (e.g., environmental stochasticity and competition removed for $\mathcal{M}_D$). 18

S2 Percent differences of synchrony of per capita growth rates between each removal simulation experiment and the 'All Drivers' simulation. 18

S3 Correlations of species' year random effects for each site by term, where term refers to the random effect on the slope or the intercept. 19

S4 Average interaction coefficients for each vital rate for each community. 19

S5 Interaction coefficients for growth regressions in Arizona. 19

S6 Interaction coefficients for survival regressions in Arizona. 20

S7 Interaction coefficients for recruitment regressions in Arizona. 20

S8 Interaction coefficients for growth regressions in Idaho. 20

S9 Interaction coefficients for survival regressions in Idaho. 21

S10 Interaction coefficients for recruitment regressions in Idaho. 21

S11 Interaction coefficients for growth regressions in Kansas. 21

S12 Interaction coefficients for survival regressions in Kansas. 22

S13 Interaction coefficients for recruitment regressions in Kansas. 22

S14 Interaction coefficients for growth regressions in Montana. 22

S15 Interaction coefficients for survival regressions in Montana. 23

S16 Interaction coefficients for recruitment regressions in Montana. 23

S17 Interaction coefficients for growth regressions in NewMexico. 23

S18 Interaction coefficients for survival regressions in NewMexico. 24

S19 Interaction coefficients for recruitment regressions in NewMexico. 24

Derivation of limiting case predictions for synchrony of per capita growth rates (Equations 3-4)

Following Loreau and de Mazancourt (2013) and de Mazancourt et al. (2013), we define population growth, ignoring observation error, as

$$r_i(t) = r_{mi}\left[1 - \frac{N_i(t) + \sum_{j\neq i}\alpha_{ij}N_j(t)}{K_i} + \sigma_{ei}u_{ei}(t) + \frac{\sigma_{di}u_{di}(t)}{\sqrt{N_i(t)}}\right] \tag{S1}$$

where $N_i(t)$ is the biomass of species *i* in year *t*, and $r_i(t)$ is its growth rate in year *t*. r_{mi} is species *i*'s intrinsic rate of increase, K_i is its carrying capacity, and α_{ij} is the interspecific competition coefficient representing the effect of species *j* on species *i*. Environmental stochasticity is incorporated as $\sigma_{ei}u_{ei}(t)$, where σ_{ei}^2 is the environmental variance and u_{ei} are normal random variables with zero mean and unit variance that are independent through time but may be correlated between species. Demographic stochasticity arises from variations in births and deaths among individuals (e.g., same states, different fates), and is included in the model as a first order, normal approximation (Lande et al. 2003, de Mazancourt et al. 2013). σ_{di}^2 is the demographic variance and $u_{di}(t)$ are independent normal variables with zero mean and unit variance.

First-order approximations of the temporal variance of total community biomass are obtained as follows (Ives 1995, Hughes and Roughgarden 2000, Ives and Hughes 2002, Loreau and de Mazancourt 2008, de Mazancourt et al. 2013). Let $\delta N_i(t) = N_i(t) - N_i^*$ denote the deviation of observed species *i*'s biomass from its equilibrium value in the community, N_i^*, in the absence of stochasticity. Equation (S1) can be Taylor expanded around $\delta N_i(t) = u_{ei}(t) = u_{di}(t) = u_{oi}^S(t) = 0$ to yield, after dropping terms of order two and higher,

$$\boldsymbol{\delta}\mathbf{N}(t+1) = \mathbf{A}\boldsymbol{\delta}\mathbf{N}(t) + \mathbf{z}(t), \tag{S2}$$

where $\boldsymbol{\delta}\mathbf{N}(t)$ is the vector of deviations of species biomasses from their deterministic equilibrium value, $\mathbf{A}$ is the community matrix, also known as the Jacobian matrix around the equilibrium, with elements $(a_{ij})_{1<i,j<S}$:

$$A_{ij} = \begin{cases} 1 - r_{mi}\frac{N_i^*}{K_i}, & i = j \\ -r_{mi}\frac{N_i^*}{K_i}\alpha_{ij}, & i \neq j \end{cases} \tag{S3}$$

and $\mathbf{z}(t)$ is a vector that encapsulates the effects of environmental and demographic stochasticity whose elements are

$$z_i(t) = N_i^*\sigma_{ei}u_{ei}(t) + \sqrt{N_i^*}\sigma_{di}u_{di}(t) \tag{S4}$$

When the system reaches a stationary distribution, the variances and covariances between species biomass time series are:

$$\left\langle \boldsymbol{\delta}\mathbf{N}(t)\boldsymbol{\delta}\mathbf{N}(t)^T \right\rangle = \mathbf{C}^{\infty} = (\mathrm{cov}(N_i, N_j))_{1<i,j<S} = (\mathrm{cov}(\delta N_i, \delta N_j))_{1<i,j<S} \tag{S5}$$

where $\boldsymbol{\delta}\mathbf{N}^T$ is the transpose of vector $\boldsymbol{\delta}\mathbf{N}$, i.e. a row vector.

Our assumptions listed above lead to the following correlation structure of $\mathbf{z}$:

$$\left\langle \mathbf{z}(t)\mathbf{z}(t)^T \right\rangle = \mathbf{B} \tag{S6}$$

$$\left\langle \mathbf{z}(t-s)\mathbf{z}(t)^T \right\rangle = 0 \qquad \text{for } s > 0 \tag{S7}$$

We use Equation S2 to write a dynamical equation for the covariance $\mathbf{C}$:

$$\begin{aligned}
\mathbf{C}(t+1) =& \left\langle \boldsymbol{\delta}\mathbf{N}(t+1)\boldsymbol{\delta}\mathbf{N}(t+1)^T \right\rangle && \text{(S8)}\\
=& \mathbf{A}\left\langle \boldsymbol{\delta}\mathbf{N}(t)\boldsymbol{\delta}\mathbf{N}(t)^T \right\rangle \mathbf{A}^T + \mathbf{A}\left\langle \boldsymbol{\delta}\mathbf{N}(t)\boldsymbol{\delta}\mathbf{N}(t)^T \right\rangle + \left\langle \mathbf{z}(t)\boldsymbol{\delta}\mathbf{N}(t)^T \right\rangle \mathbf{A}^T + \left\langle \mathbf{z}(t)\mathbf{z}(t)^T \right\rangle && \text{(S9)}\\
=& \mathbf{A}\mathbf{C}(t)\mathbf{A}^T + \mathbf{Z}_0 && \text{(S10)}
\end{aligned}$$

Taking the limit $t \to \infty$ on both sides, we get:

$$\mathbf{C}^{\infty} = \mathbf{A}\mathbf{C}^{\infty}\mathbf{A}^T + \mathbf{B} \tag{S11}$$

where $\mathbf{A}$ is as in Equation S3 and $\mathbf{B}$ is:

$$B_{ij} = N_i^* N_j^* \sigma_{ei}\sigma_{ej}\mathrm{cov}(u_{ei}, u_{ej}) + \sqrt{N_i^* N_j^*}\sigma_{di}\sigma_{dj}\mathrm{cov}(u_{di}, u_{dj}) \tag{S12}$$

Similarly, $\mathbf{R}$ is the variance-covariance matrix for population growth rates at steady state

$$R_{ij} = \frac{r_{mi}r_{mj}}{K_i K_j}\sum_{k,l}\alpha_{ik}\alpha_{jl}C_{kl} + \sigma_{ei}\sigma_{ej}\mathrm{cov}(u_{ei}, u_{ej}) + \frac{\sigma_{di}\sigma_{dj}\mathrm{cov}(u_{di}, u_{dj})}{\sqrt{N_i^* N_j^*}}. \tag{S13}$$

Then, following the synchrony metric of Loreau and de Mazancourt (2008), the sychrony of population biomasses is

$$\phi_N = \frac{\sum_{i,j} C_{ij}}{\left(\sum_i \sqrt{C_{ii}}\right)^2} \tag{S14}$$

and the synchrony of per capita growth rates is

$$\phi_R = \frac{\sum_{i,j} R_{ij}}{\left(\sum_i \sqrt{R_{ii}}\right)^2}. \tag{S15}$$

Synchrony of population biomasses and growth rates emerge from complex interactions among species' intrinsic growth rates, interspecific interactions, environmental stochasticity, and demographic stochasticity. Given these complexities, it is impossible to determine expected effects of different parameters in a multi-species case. Thus, we analyze a simplified case where interspecific interactions are zero. The variance-covariance matrix of population biomasses at steady state then becomes

$$c_{ij} = \frac{B_{ij}}{1 - A_i i A_j j} = \frac{N_i^* N_j^* \sigma_{ei}\sigma_{ej}\text{cov}(u_{ei}, u_{ej}) + \sqrt{N_i^* N_j^*}\sigma_{di}\sigma_{dj}\text{cov}(u_{di}, u_{dj})}{1 - (1 - r_{mi})(1 - r_{mj})} \tag{S16}$$

and the variance-covariance matrix of population growth rates simplifies to

$$R_{ij} = \frac{1}{1 - \frac{r_{mi} r_{mj}}{r_{mi} + r_{mj}}} \left(\sigma_{ei}\sigma_{ej}\text{cov}(u_{ei}, u_{ej}) + \frac{\sigma_{di}\sigma_{dj}\text{cov}(u_{di}, u_{dj})}{\sqrt{N_i^* N_j^*}} \right) \tag{S17}$$

Note that synchrony in population sizes and synchrony in growth rates use weighted factors of the environmental variances and covariances with species-specific parameters. So, we further assume that, along with interspecific interactions being zero, all species have identical growth rates, environmental stochasticity is absent, and all species have identical demographic variance. This represents a theoretical limiting case where the community consists of identical species coexisting in a constant environment where only demographic stochasticity causes temporal fluctuations. Under such conditions, synchrony of population biomasses is

$$\phi_N = \frac{1}{\left(\sum_i p_i^{1/2}\right)^2} \tag{S18}$$

and synchrony of growth rates is

$$\phi_R = \frac{\sum_i p_i^{-1}}{\left(\sum_i p_i^{-1/2}\right)^2} \tag{S19}$$

where p_i is the average frequency of species *i*, $p_i = N_i/N_T$. When all species have identical abundances and $p_i = 1/S$, where *S* is species richness, the both synchrony values equal 1/S (Loreau and de Mazancourt 2008). The prediction represented in Equation S19 is Equation 3 in the main text, which we refer to as $\phi_{R,\mathcal{M}_D}$.

Another limiting case is where only environmental stochasticity is operating: no interspecific interactions, no demographic stochasticity, identical intrinsic growth rates, and environmental stochasticity with same standard deviation for all species. Under such constraints, the synchrony of of species' biomasses is

$$\phi_N = \sum_{i,j} p_i p_j \text{cov}(u_{ei}, u_{ej}) \tag{S20}$$

and the synchrony of species' growth rates is

$$\phi_R = \frac{\sum_{i,j} \mathrm{cov}(u_{ei}, u_{ej})}{S^2} \tag{S21}$$

The prediction represented in Equation S21 is Equation 4 in the main text, which we refer to as $\phi_{R,\mathcal{M}_E}$. If we know the covariance matrix of the species environmental responses, we can calculate the above expectations directly. Note that the environmental responses are normalized in the above equations, therefore the covariances are correlations in the above equations.

Materials and methods details

Vital rate statistical models

We modeled survival probability and growth on individual genets as a function of genet size, the crowding experienced by the focal genet from both heterospecific and conspecific genets in its neighborhood (described below), temporal varation among years, and spatial variation among quadrat groups. Groups are sets of quadrats located in close proximity within a pasture or grazing exclosure.

We follow the approach of Chu and Adler (2015) to estimate crowding, assuming that the crowding experienced by a focal genet depends on distance to each neighbor genet and the neighbor's size, *u*:

$$w_{ijm,t} = \sum_k e^{-\delta_{jm} d^2_{ijkm,t}} u_{km,t}. \tag{S22}$$

In the above, $w_{ijm,t}$ is the crowding that genet *i* of species *j* in year *t* experiences from neighbors of species *m*. The spatial scale over which species *m* neighbors exert influence on any genet of species *j* is determined by δ_{jm}. The function is applied for all *k* genets of species *m* that neighbor the focal genet at time *t*, and $d_{ijkm,t}$ is the distance between genet *i* in species *j* and genet *k* in species *m*. When $k = m$, the effect is intraspecific crowding. We use regression-specific (survival and growth) δ values estimated by Chu and Adler (2015).

We used logistic regression to model survival probability (S) of genet i from species j in quadrat group g from time t to $t + 1$:

$$\text{logit}(S_{ijg,t}) = \gamma^S_{j,t} + \phi^S_{jg} + \beta^S_{j,t} x_{ij,t} + \boldsymbol{\omega}^S_j \mathbf{w}_{ij,t} \tag{S23}$$

where $x_{ij,t}$ is the log of genet size, $\gamma^S_{j,t}$ is a year-specific intercept, $\beta^S_{j,t}$ is the year-specific slope parameter for size, ϕ^S_{jg} is the random effect of quadrat group location, and ω is a vector of per capita interaction coefficients which determine the impact of crowding, **w**, by each species on the focal species.

We modeled genet growth, conditional on survival, in a similar manner:

$$\mu_{ijg,t+1} = \gamma^G_{j,t} + \phi^G_{jg} + \beta^G_{j,t} \mu_{ij,t} + \boldsymbol{\omega}^G_j \mathbf{w}_{ij,t} \tag{S24}$$

where μ is log genet size and all other parameters are as described for the survival regression. We capture non-constant error variance in growth by modeling the variance around the growth regression (ε) as a nonlinear function of predicted genet size:

$$\varepsilon_{ij,t} = a e^{b \mu_{ijg,t+1}} \tag{S25}$$

Our data allows us to track new recruits, but we cannot assign a specific parent to new genets. THerefore, we model recruitment at the quadrat level: the number of new individuals of species j in quadrat q recruiting at time $t+1$ as a function of quadrat "effective cover" (A') in the previous year (t). Effective cover is a mixture of observed cover (A) in the focal quadrat (q) and the mean cover across the entire group ($\bar{A}$) of Q quadrats in which q is located:

$$A'_{jq,t} = p_j A_{jq,t} + (1 - p_j)\bar{A}_{jQ,t} \tag{S26}$$

where p is a mixing fraction between 0 and 1 that is estimated within the model.

We assume the number of individuals, y^R, recruiting at time $t+1$ follows a negative binomial distribution:

$$y^R_{jq,t+1} \sim \text{NegBin}(\lambda_{jq,t+1}, \zeta) \tag{S27}$$

where λ is the mean intensity and ζ is the size parameter. We define λ as:

$$\lambda_{jq,t+1} = A'_{jq,t} e^{(\gamma^R_{j,t} + \phi^R_{jQ} + \theta^R_{jk} C_{k,t} + \omega^R \sqrt{A'_{q,t}})} \tag{S28}$$

where A' is effective cover (cm^2) of species j in quadrat q and all other terms are as in the survival and growth regressions.

Multi-species populations models

The individually based model (IBM) is straighforward and described in the main text, so here focus on the structure of the integral projeciton model (IPM). We built an environmentally stochastic IPM. Our IPM follows the specification of Chu and Adler (2015) where the population of species *j* is a density function $n(u_j, t)$ giving the density of sized-*u* genets at time *t*. Genet size is on the natural log scale, so that $n(u_j, t)du$ is the number of genets whose area (on the arithmetic scale) is between e^{u_j} and $e^{u_j + du}$. So, the density function for any size *v* at time $t+1$ is

$$n(v_j, t+1) = \int_{L_j}^{U_j} k_j(v_j, u_j, \bar{\mathbf{w}}_\mathbf{j}(u_j)) n(u_j, t) \tag{S29}$$

where $k_j(v_j, u_j, \bar{\mathbf{w}}_\mathbf{j})$ is the population kernal that describes all possible transitions from size u to v and $\bar{\mathbf{w}}_\mathbf{j}$ is a vector of estimates of average crowding experienced from all other species by a genet of size u_j and species j. The integral is evaluated over all possible sizes between predefined lower (*L*) and upper (*U*) size limits that extend beyond the range of observed genet sizes.

The population kernal is defined as the joint contributions of survival (*S*), growth (*G*), and recruitment (*R*):

$$k_j(v_j, u_j, \bar{\mathbf{w}}_\mathbf{j}) = S_j(u_j, \bar{\mathbf{w}}_\mathbf{j}(u_j)) G_j(v_j, u_j, \bar{\mathbf{w}}_\mathbf{j}(u_j)) + R_j(v_j, u_j, \bar{\mathbf{w}}_\mathbf{j}), \tag{S30}$$

which means we are calculating growth (*G*) for individuals that survive (*S*) from time *t* to *t+1* and adding in newly recruited (*R*) individuals of an average sized one-year-old genet for the focal species. Our stastical model for recruitment (*R*, described below) returns the number of new recruit produced per quadrat. Following previous work, we assume that fecundity increases linearly with size ($R_j(v_j, u_j, \bar{\mathbf{w}}_\mathbf{j}) = e^{u_j} R_j(v_j, \bar{\mathbf{w}}_\mathbf{j})$) to incorporate the recruitment function in the spatially-implicit IPM.

Results for synchrony of percent cover

Synchrony of percent cover from population model simulations did not compare well with observed synchrony of cover or analytical predictions for synchrony cover (Fig. S2, S3). We did not expect synchrony of percent cover from simulations to compare well with observed synchrony of cover because our models represent equilibrium dynamics rather than a specific set of observed years. Also, unlike growth rates, synchrony in cover is highly influenced by drift and legacy effects (Loreau and de Mazancourt 2008).

More interesting is that our simulation results did not compare well with analytical predictions. One issue is that some species are not well-regulated around their equilibrium cover, so that our linear approximation required for anayltical predictions is likely to fail. Analytical predictions for synchrony of growth rates are more informative than synchrony in population sizes because the linear approximation is more proximate.

Another issue is the influence of demographic stochasticity in some communities, for example, in Idaho where our simulations with only demographic stochasticity yielded results far different from analytical predicitons (Fig. S2). Our analytical predictions require the unrealistic assumption that demographic variances among species are equal. However, in Idaho, *A. tripartita* has much higher demographic stochasticity than the other species, so that variation in its abundance dominates. Thus, the assumption that all species have similar stochasticity fails. In combination, our results from analyzing synchrony of percent cover indicate that the best way to decipher the mechanisms contributing to community synchrony is to analyze growth rates, in agreement with the theoretical arguments of Loreau and de Mazancourt (2008).

Supporting Figures

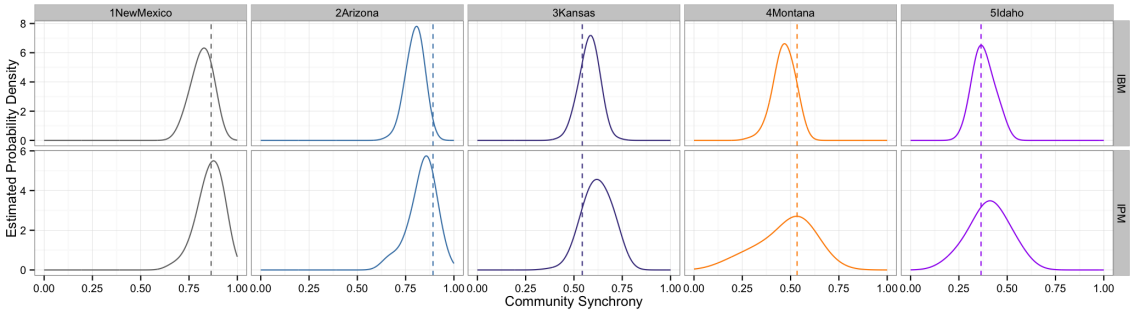

Figure S1: Observed (vertical dashed lines) and simulated (solid density curves) synchrony of species per capita growth rates at each site from the IBM (top panels) and the IPM (bottom panels). IPM density curves come from 100 random contiguous sections from 2,000 iteration IPM runs, where the length of each randomly selected section is equal to the number of observation years for each data set. IBM density curves come from 100 replicate simulations of 75 iterations each. Synchrony values come from simulations where environmental stochasticity and interspecific interactions are present. The IBM was run on a 5 by 5 meter landscape to reduce the effect of demographic stochasticity.

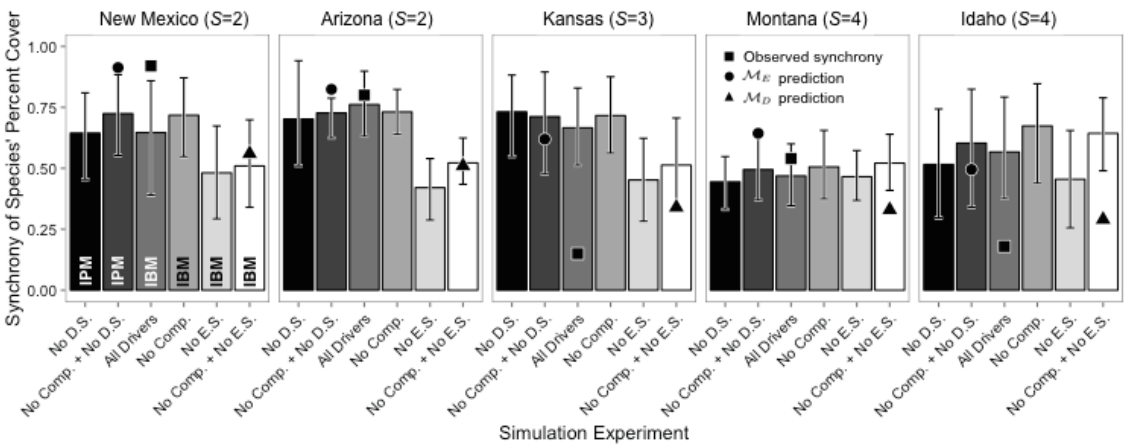

Figure S2: Community-wide synchrony of species percent cover from model simulation experiments. Synchrony of species' percent cover for each study area are from simulation experiments with demographic stochasticity, environmental stochasticity, and interspecific competition present ("All Drivers"), demographic stochasticity removed ("No D.S."), environmental stochasticity removed ("No E.S."), interspecific competition removed ("No Comp."), interspecific competition and demographic stochasticity removed ("No Comp. + No D.S."), and interspecific competition and environmental stochasticity removed ("No Comp. + No E.S."). Abbreviations within the bars for the New Mexico site indicate whether the IBM or IPM was used for a particular simulation. Error bars represent the 2.5% and 97.5% quantiles from model simulations.

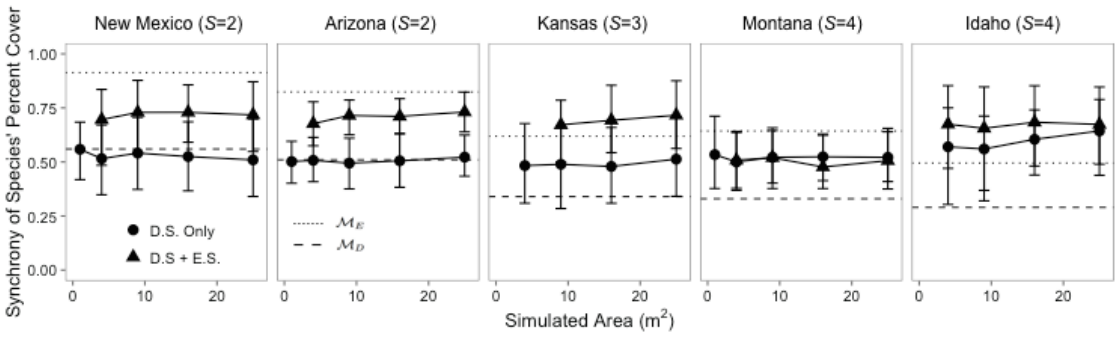

Figure S3: Synchrony of species' percent cover for each study area from IBM simulations across different landscape sizes when only demographic stochastcity is present ("D.S. Only") and when environmental stochasticity is also present removed ("D.S. + E.S."). The horizontal lines show the analytical predictions $\mathcal{M}_D$ (dashed line) and $\mathcal{M}_E$ (dotted line). The strength of demographic stochasticity decreases as landscape size increases because population sizes also increase. Error bars represent the 2.5% and 97.5% quantiles from model simulations.

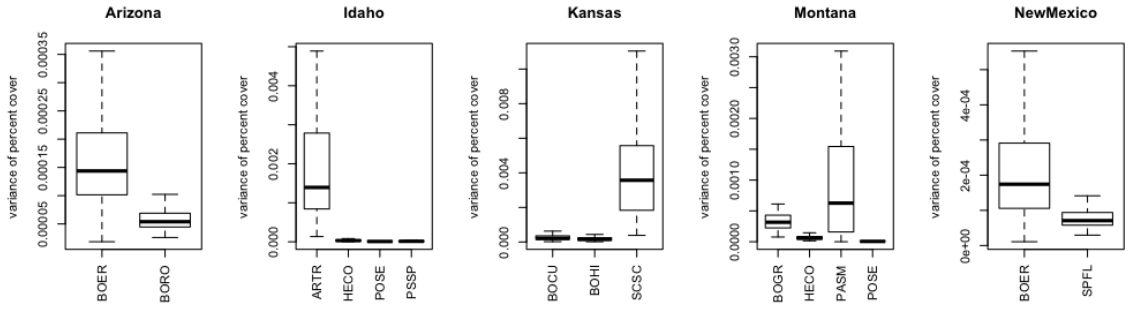

Figure S4: Variance of percent cover for each species (along x-axes) in each site through time from simulations with only environmental stochasticity operating (IPM with no species interactions).

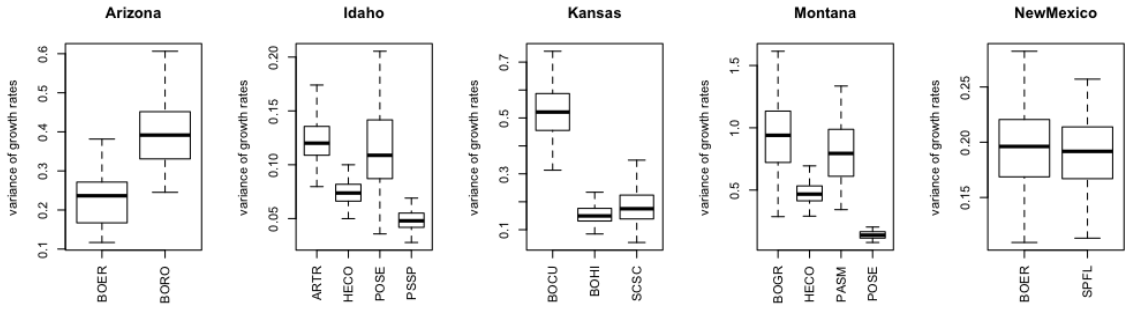

Figure S5: Variance of per capita growth rates for each species (along x-axes) in each site through time from simulations with only environmental stochasticity operating (IPM with no species interactions).

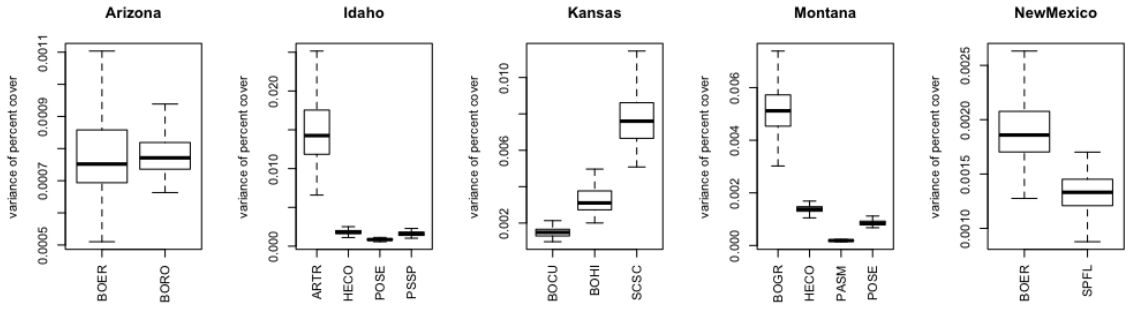

Figure S6: Variance of percent cover for each species (along x-axes) in each site through time from simulations with only demographic stochasticity operating (IBM simulated on 5 by 5 meter landscape).

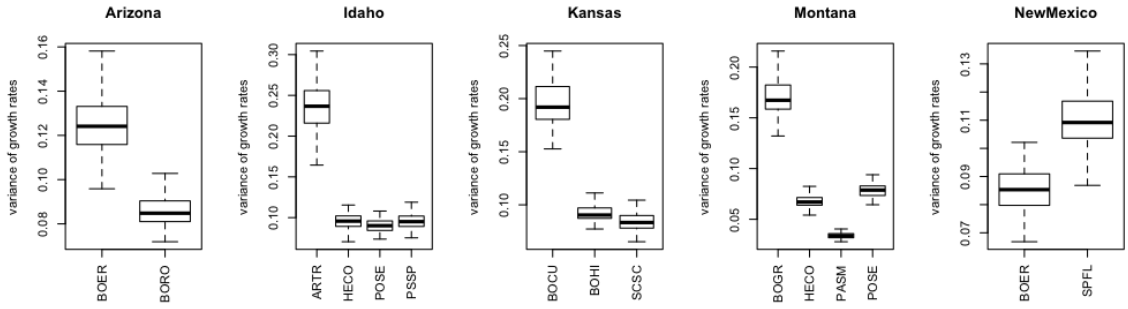

Figure S7: Variance of per capita growth rates for each species (along x-axes) in each site through time from simulations with only demographic stochasticity operating (IBM simulated on 5 by 5 meter landscape).

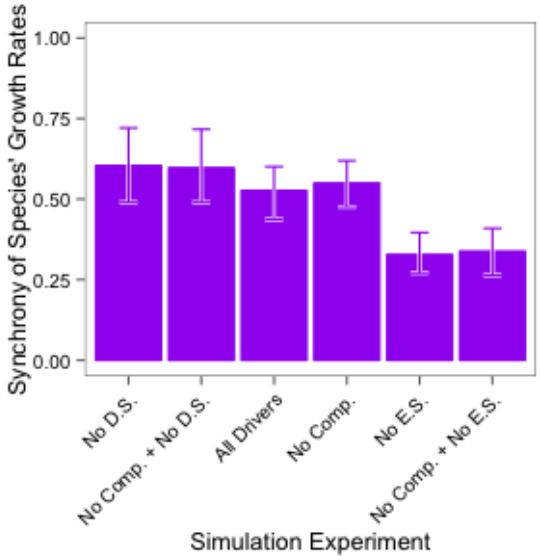

Figure S8: Community-wide synchrony of species' growth rates from model simulation experiments for the Idaho community with *Artemisia tripartita* removed. Synchrony of species' growth rates are from simulation experiments with demographic stochasticity, environmental stochasticity, and interspecific competition present ("All Drivers"), demographic stochasticity removed ("No D.S."), environmental stochasticity removed ("No E.S."), interspecific competition removed ("No Comp."), interspecific competition and demographic stochasticity removed ("No Comp. + No D.S."), and interspecific competition and environmental stochasticity removed ("No Comp. + No E.S."). Error bars represent the 2.5% and 97.5% quantiles from model simulations.

Supporting Tables

In all tables, species codes are as follows (also see Table 1 in the main text):

- *Bouteloua eriopoda* = BOER
- *Sporobolus flexuosus* = SPFL
- *Bouteloua rothrockii* = BORO
- *Bouteloua curtipendula* = BOCU
- *Bouteloua hirsuta* = BOHI
- *Schizachyrium scoparium* = SCSC
- *Bouteloua gracilis* = BOGR
- *Hesperostipa comata* = HECO
- *Pascopyrum smithii* = PASM
- *Poa secunda* = POSE
- *Artemisia tripartita* = ARTR
- *Pseudoroegneria spicata* = PSSP

Table S1: Comparisons between our analytical predictions and simulation results for synchrony of species' per capita growth rates. Analytical predictions represent two limiting cases where only demographic stochasticity is operating ($\phi_{R,\mathcal{M}_D}$) and where only environmental stochasticity is operating ($\phi_{R,\mathcal{M}_E}$). Simulated synchrony values come from our empirically-based, multi-species population models when simulated under conditions that match the limiting case conditions (e.g., environmental stochasticity and competition removed for $\mathcal{M}_D$).

Site	Predicted $\phi_{R,\mathcal{M}_D}$	Simulated $\phi_{R,\mathcal{M}_D}$	Predicted $\phi_{R,\mathcal{M}_E}$	Simulated $\phi_{R,\mathcal{M}_E}$
New Mexico	0.56	0.51	0.86	0.86
Arizona	0.51	0.52	0.82	0.81
Kansas	0.35	0.39	0.62	0.62
Montana	0.31	0.31	0.47	0.50
Idaho	0.29	0.31	0.43	0.42

Table S2: Percent differences of synchrony of per capita growth rates between each removal simulation experiment and the 'All Drivers' simulation.

simulation	1New Mexico	2Arizona	3Kansas	4Montana	5Idaho
1No D.S.	5.53	4.28	6.01	5.27	11.95
2No Comp. + No D.S.	5.56	2.06	7.03	6.21	9.10
4No Comp.	0.98	0.06	4.84	1.43	0.11
5No E.S.	40.14	33.20	47.84	39.06	9.28
6No Comp. + No E.S.	45.95	41.48	38.21	39.44	20.33

Table S3: Correlations of species' year random effects for each site by term, where term refers to the random effect on the slope or the intercept.

site	term	growth	recruit	surv
Arizona	intercept	0.51	-0.05	0.51
Arizona	slope	0.68		0.16
Idaho	intercept	0.45	0.38	0.25
Idaho	slope	0.50		0.47
Kansas	intercept	0.44	0.29	0.26
Kansas	slope	0.19		0.16
Montana	intercept	0.29	0.07	0.41
Montana	slope	0.11		0.02
NewMexico	intercept	0.51	-0.15	0.65
NewMexico	slope	0.37		0.20

Table S4: Average interaction coefficients for each vital rate for each community.

Site	Interaction Type	Growth	Recruitment	Survival
Arizona	Interspecific	-0.0111	-0.4534	-0.0507
Arizona	Intraspecific	-0.0402	-1.4209	-0.4446
Idaho	Interspecific	0.0022	-0.1091	0.0059
Idaho	Intraspecific	-0.0469	-1.5569	-0.5269
Kansas	Interspecific	-0.0008	0.0463	-0.0041
Kansas	Intraspecific	-0.0062	-0.9945	-0.0586
Montana	Interspecific	-0.0059	0.0691	0.0342
Montana	Intraspecific	-0.0801	-2.0900	-0.8652
NewMexico	Interspecific	-0.0027	-0.3461	-0.0080
NewMexico	Intraspecific	-0.0111	-1.6473	-0.2191

Interaction Coefficients for Vital Rates in Arizona

Table S5: Interaction coefficients for growth regressions in Arizona.

	BOER	BORO
BOER	-0.0033	-0.0171
BORO	-0.0050	-0.0772

Table S6: Interaction coefficients for survival regressions in Arizona.

	BOER	BORO
BOER	-0.2791	-0.0814
BORO	-0.0200	-0.6102

Table S7: Interaction coefficients for recruitment regressions in Arizona.

	BOER	BORO
BOER	-0.5184	-0.3290
BORO	-0.5779	-2.3235

Interaction Coefficients for Vital Rates in Idaho

Table S8: Interaction coefficients for growth regressions in Idaho.

	ARTR	HECO	POSE	PSSP
ARTR	-0.0300	0.0129	0.0117	0.0003
HECO	-0.0000	-0.0285	0.0084	-0.0028
POSE	0.0001	0.0032	-0.0845	-0.0043
PSSP	-0.0003	-0.0027	-0.0004	-0.0448

Table S9: Interaction coefficients for survival regressions in Idaho.

	ARTR	HECO	POSE	PSSP
ARTR	-0.0236	-0.0199	0.0314	0.0158
HECO	-0.0005	-1.0206	-0.0051	0.0125
POSE	0.0001	0.0006	-0.9088	0.0121
PSSP	0.0009	-0.0013	0.0248	-0.1547

Table S10: Interaction coefficients for recruitment regressions in Idaho.

	ARTR	HECO	POSE	PSSP
ARTR	-0.4003	0.2243	0.0117	0.2360
HECO	-0.5681	-1.7594	-0.1437	-0.3195
POSE	-0.2505	-0.0131	-2.2928	-0.1420
PSSP	-0.2405	-0.1389	0.0347	-1.7751

Interaction Coefficients for Vital Rates in Kansas

Table S11: Interaction coefficients for growth regressions in Kansas.

	BOCU	BOHI	SCSC
BOCU	-0.0017	0.0011	0.0010
BOHI	0.0002	-0.0046	-0.0078
SCSC	-0.0003	0.0007	-0.0124

Table S12: Interaction coefficients for survival regressions in Kansas.

	BOCU	BOHI	SCSC
BOCU	-0.1084	0.0006	0.0010
BOHI	0.0021	-0.0403	-0.0153
SCSC	-0.0064	-0.0066	-0.0271

Table S13: Interaction coefficients for recruitment regressions in Kansas.

	BOCU	BOHI	SCSC
BOCU	-1.1544	-0.0312	-0.0643
BOHI	0.3410	-0.8681	0.0041
SCSC	0.0619	-0.0336	-0.9611

Interaction Coefficients for Vital Rates in Montana

Table S14: Interaction coefficients for growth regressions in Montana.

	BOGR	HECO	PASM	POSE
BOGR	-0.0124	-0.0032	-0.0258	-0.0001
HECO	-0.0025	-0.0976	0.0096	0.0079
PASM	-0.0006	-0.0041	-0.0695	-0.0030
POSE	0.0006	-0.0082	-0.0417	-0.1410

Table S15: Interaction coefficients for survival regressions in Montana.

	BOGR	HECO	PASM	POSE
BOGR	-0.1316	0.0076	0.1096	0.0126
HECO	-0.0028	-0.7064	0.1423	-0.0030
PASM	-0.0012	-0.0033	-1.4026	0.0024
POSE	0.0014	0.0082	0.1363	-1.2203

Table S16: Interaction coefficients for recruitment regressions in Montana.

	BOGR	HECO	PASM	POSE
BOGR	-0.9151	-0.3076	-0.0984	0.0495
HECO	-0.0785	-1.4192	-0.0480	-0.0468
PASM	-0.0103	0.2773	-4.3148	0.3470
POSE	0.1971	0.4854	0.0623	-1.7109

Interaction Coefficients for Vital Rates in New Mexico

Table S17: Interaction coefficients for growth regressions in NewMexico.

	BOER	SPFL
BOER	-0.0045	-0.0013
SPFL	-0.0041	-0.0176

Table S18: Interaction coefficients for survival regressions in NewMexico.

	BOER	SPFL
BOER	-0.1576	-0.0040
SPFL	-0.0120	-0.2806

Table S19: Interaction coefficients for recruitment regressions in NewMexico.

	BOER	SPFL
BOER	-0.7649	-0.6230
SPFL	-0.0691	-2.5296

References

Chu, C., and P. B. Adler. 2015. Large niche differences emerge at the recruitment stage to stabilize grassland coexistence. Ecological Monographs 85:373–392.

de Mazancourt, C., F. Isbell, A. Larocque, F. Berendse, E. De Luca, J. B. Grace, B. Haegeman, H. Wayne Polley, C. Roscher, B. Schmid, D. Tilman, J. van Ruijven, A. Weigelt, B. J. Wilsey, and M. Loreau. 2013. Predicting ecosystem stability from community composition and biodiversity. Ecology Letters 16:617–625.

Hughes, J. B., and J. Roughgarden. 2000. Species Diversity and Biomass Stability. The American Naturalist 155:618–627.

Ives, A. 1995. Predicting the Response of Populations to Environmental Change. Ecology 76:926–941.

Ives, A. R., and J. B. Hughes. 2002. General Relationships Between Species Diversity and Stability in Competitive Systems. The American Naturalist 159:388–395.

Lande, R., S. Engen, and B.-E. Saether. 2003. Stochastic population dynamics in ecology and conservation.

Loreau, M., and C. de Mazancourt. 2008. Species synchrony and its drivers: neutral and nonneutral community dynamics in fluctuating environments. The American Naturalist 172:E48–E66.

Loreau, M., and C. de Mazancourt. 2013. Biodiversity and ecosystem stability: A synthesis of underlying mechanisms. Ecology Letters 16:106–115.